

## Research Paper

**Cite this article:** Jin X, Xiong K, Marstell R, Strandwitz NC, Hwang JCM, Farina M, Göritz A, Wietstruck M, Kaynak M (2018). Scanning microwave microscopy of buried CMOS interconnect lines with nanometer resolution. *International Journal of Microwave and Wireless Technologies* **10**, 556–561. <https://doi.org/10.1017/S1759078718000181>

Received: 14 September 2017  
Revised: 10 January 2018  
Accepted: 11 January 2018  
First published online: 17 April 2018

### Key words:

Microwave measurements; semiconductor devices and IC-technologies; interaction of EM waves with matter

### Author for correspondence:

Xin Jin, E-mail: [xij215@lehigh.edu](mailto:xij215@lehigh.edu)

# Scanning microwave microscopy of buried CMOS interconnect lines with nanometer resolution

Xin Jin<sup>1</sup>, Kuanchen Xiong<sup>1</sup>, Roderick Marstell<sup>1</sup>, Nicholas C. Strandwitz<sup>1</sup>, James C. M. Hwang<sup>1</sup>, Marco Farina<sup>2</sup>, Alexander Göritz<sup>3</sup>, Matthias Wietstruck<sup>3</sup> and Mehmet Kaynak<sup>3</sup>

<sup>1</sup>Lehigh University, Bethlehem, Pennsylvania 18015, USA; <sup>2</sup>Marche Polytechnic University, Ancona 60131, Italy and <sup>3</sup>IHP, Im Technologiepark 25, 15236, Frankfurt (Oder), Germany

This paper reports scanning microwave microscopy of CMOS interconnect aluminum lines both bare and buried under oxide. In both cases, a spatial resolution of  $190 \pm 70$  nm was achieved, which was comparable or better than what had been reported in the literature. With the lines immersed in water to simulate high- $k$  dielectric, the signal-to-noise ratio degraded significantly, but the image remained as sharp as before, especially after averaging across a few adjacent scans. These results imply that scanning microwave microscopy can be a promising technique for non-destructive nano-characterization of both CMOS interconnects buried under oxide and live biological samples immersed in water.

## Introduction

A state-of-the-art CMOS chip comprises not only billions of transistors, but also 10 or more levels of nanometer-to-micrometer-wide metal lines buried in interlevel oxides to interconnect the transistors [1]. For quality control and failure analysis, it is a challenge to inspect these interconnect lines that crisscross through the oxides. For this purpose, although X-ray or electron microscopy can be used, they can damage the oxides. Traditional scanning probes such as atomic force microscope (AFM) and scanning tunneling microscope (STM) can provide nanometer resolution non-destructively. However, they are sensitive only to surface properties. In comparison, scanning microwave microscope (SMM), an emerging derivative of AFM or STM, can penetrate up to a micrometer in oxides and other dielectrics [2]. Additionally, being sensitive to electrical properties, SMM shows sharp contrast between metal and dielectric. SMM achieves nanometer resolution through near-field interaction between the nanometer probe and the sample, despite the relatively large microwave wavelength. SMM is non-destructive because the energy of the microwave photons is on the order of 10  $\mu$ eV.

Recently, SMM was successfully used to image 1.2  $\mu$ m-wide Al-Si-Cu lines buried under plasma-deposited tetraethylorthosilicate either 800 or 2300 nm thick with  $900 \pm 70$  and  $1200 \pm 260$  nm spatial resolution, respectively [3]. Most recently, SMM was used to image 80  $\mu$ m-wide TiN-Ti-Al lines buried under atomic-layer deposited (ALD) aluminum oxide 20 nm thick with 600 nm sharpness [4]. The experiment was repeated in water to simulate high- $k$  dielectric and found the sharpness degraded by approximately 60%. This paper reports SMM of TiN-Ti-Al lines buried under 20 nm-thick ALD aluminum oxide with  $190 \pm 70$  nm resolution both in and out of water. The reason for such significant improvement is detailed below.

## Experimental setup

TiN-Ti-capped Al interconnect lines approximately 0.5  $\mu$ m thick were fabricated by a state-of-the-art 130 nm SiGe BiCMOS process on a 200 mm-diameter high-resistivity (10 k $\Omega$ .cm) Si wafer [5]. Lines with designed widths of 160 and 360 nm (actual widths 190 and 390 nm due to process bias as determined by SMM) were embedded in 1.3  $\mu$ m thick SiO<sub>2</sub>, then chemo-mechanically polished to a flatness of approximately 70 nm as indicated by the AFM profile in Fig. 1. Thereafter the wafer was diced into 25 mm  $\times$  15 mm chips. To simulate buried interconnect lines, some of the chips were coated with 20 nm of ALD Al<sub>2</sub>O<sub>3</sub> at 300 °C. The conforming ALD did not alter the surface topography significantly (Fig. 1(b)), which minimizes the so-called “topography cross-talk” difference in SMM [2] between samples with and without oxide coating. Otherwise, the SMM contrast between the two sets of samples would have been complicated by the difference in topography through its influence on the parasitic capacitance with the probe. Defining the image sharpness by the transition width from 25 to 75% height [3], Fig. 1(b) shows also that the AFM sharpness

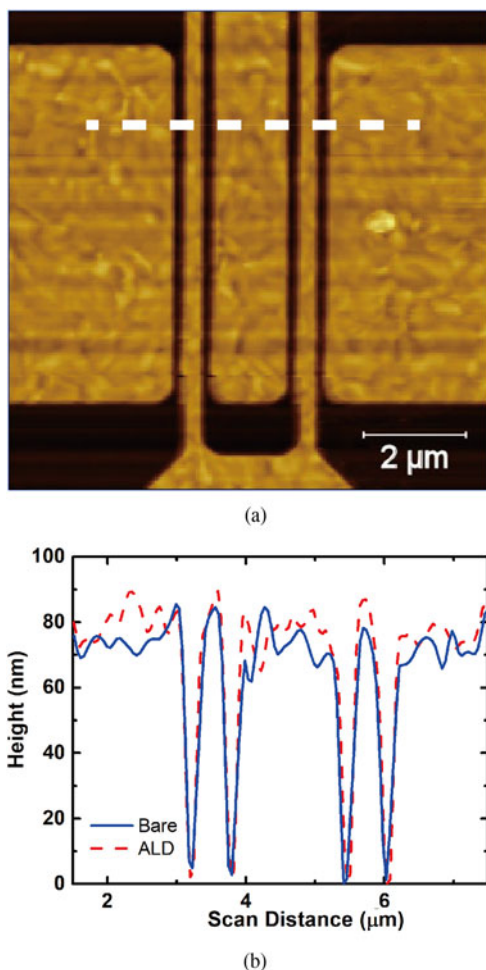


**Fig. 1.** AFM (a) image and (b) linear scan of 190 nm-wide bare (—) aluminum lines. The image of buried lines is visually indistinguishable from that of bare lines and, hence, not shown. The profile of the buried lines is also very similar to that of bare lines as indicated by dashed line (- - -) in (b). Dashed line in (a) indicates where linear scans were taken.

is approximately 80 nm, which is actually inferior to that of SMM, because the AFM scan parameters were not fully optimized giving the emphasis on SMM in this study.

The two sets of chips, with and without oxide coating, provided a good contrast between bare and buried metal lines. The aluminum lines on the uncoated chips were prevented from oxidation by TiN. The TiN and Ti layers, being nanometer thin, did not significantly change the electrical properties of the metal lines from that of pure Al. For tests in water, the chips were placed on the bottom of a petri dish that is filled with approximately 5 mm of deionized water, sufficient to immerse both the chips and the SMM probe, including its cantilever body for optical detection of the AFM deflection. The dielectric constant of deionized water was taken to be 70 according to the literature [6]. The dielectric constants of  $\text{Al}_2\text{O}_3$  and  $\text{SiO}_2$  were measured to be approximately 7 and 4, respectively, from specially made metal-insulator-metal test structures by using an Agilent Technologies 4294A precision impedance analyzer. These dielectric constants would be valuable for in-depth data analysis.

Two chips, with bare and buried lines, respectively, were mounted side-by-side on the piezoelectric stage of a Keysight Technologies Series 7500 AFM/SPM system with a N9545C SMM nose cone. Typically, topography and microwave reflection coefficient ( $S_{11}$ ) were simultaneously measured during the same scan, and their changes plotted either in one-dimensional linear scans or two-dimensional images. Figure 2 shows the present SMM setup with the microwave signal channeled to a sharp probe for near-field interaction with the chip under test. The probe comprises a Rocky Mountain 12Pt400A full-metal platinum/iridium tip with 80  $\mu\text{m}$  length and <20 nm radius, which was attached to a 400  $\mu\text{m}$ -long, 60  $\mu\text{m}$ -wide cantilever. With a spring constant of 0.3 N/m, the probe was sufficiently soft for direct contact with the chips. An Agilent Technologies N5230A PNA-L vector network analyzer (VNA) provided the microwave signal through an impedance matching network comprising a shunt resistor and coaxial cables. Typically, an input power of -5 dBm was generated at 5.371 GHz at which frequency the network was matched to the 50  $\Omega$  system impedance resulting in

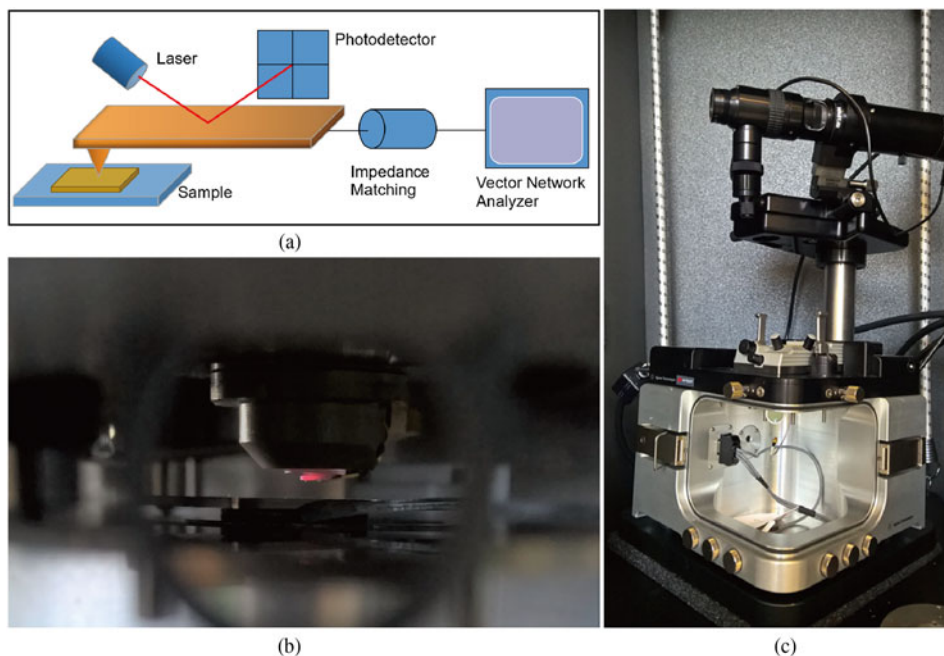
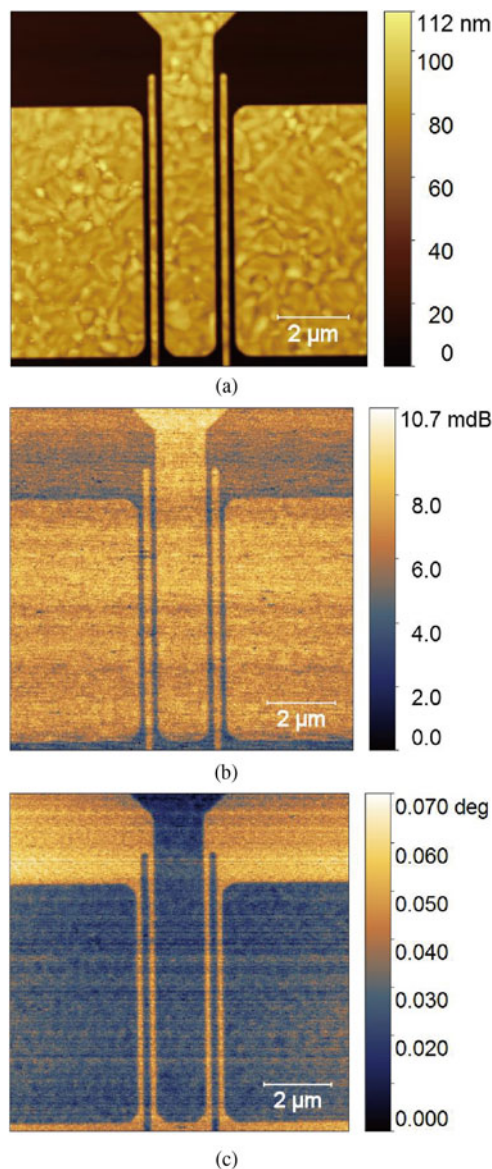


**Fig. 2.** (a) Schematic, (b) nose cone, and (c) stage of the present SMM setup.

optimum signal-to-noise ratio (SNR). The magnitude and phase of  $S_{11}$  were measured by the VNA after passing through a 30 dB preamplifier. The scan size was typically  $10\ \mu\text{m} \times 10\ \mu\text{m}$  divided into  $256 \times 256$  pixels. The SMM scan rate was limited to approximately 10 ms per pixel, because an intermediate frequency bandwidth of 1 kHz was used on the VNA for the optimum tradeoff between speed and SNR.

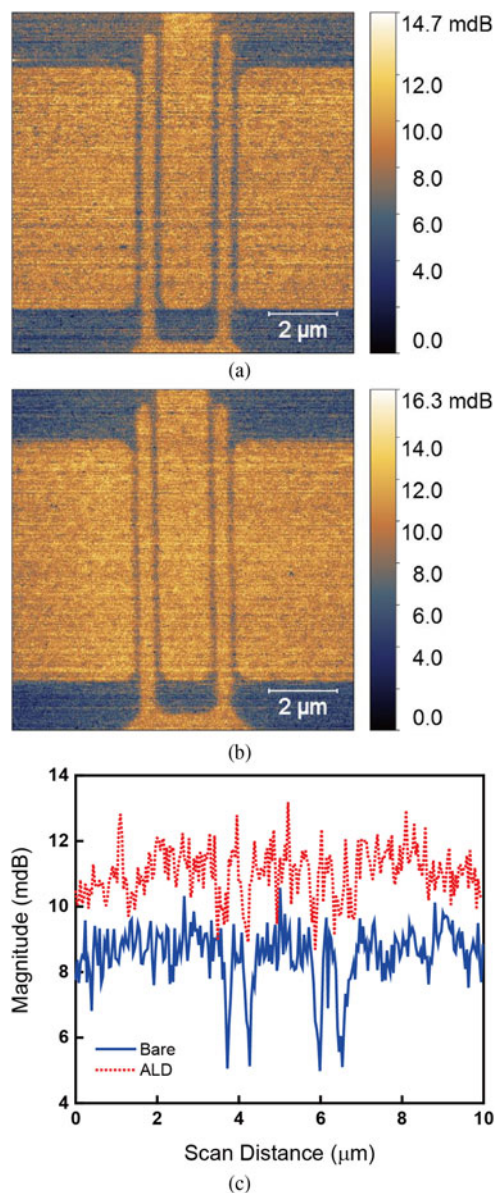
## Results and discussion

Figure 3 shows images formed simultaneously by AFM and SMM of 190 nm-wide bare aluminum lines. Whether an SMM image was formed by using the magnitude or phase of  $S_{11}$ , it appears to have comparable contrast and sharpness to that of AFM. In reality, the SNR of SMM is not as good as that of AFM due to weak SMM signals. For example, in the present case, the contrast in  $S_{11}$  magnitude and phase are on the order of 0.01 dB (10 mdB) and  $0.1^\circ$ , respectively, comparable to that previously reported [3].



**Fig. 3.** Simultaneous (a) AFM, (b) SMM magnitude, (c) SMM phase images of 190 nm-wide bare aluminum lines.

Figures 4(a) and 4(b) show SMM magnitude images of 390 nm-wide bare and buried aluminum lines, respectively. It can be seen that, even when buried under 20 nm  $\text{Al}_2\text{O}_3$ , the lines are clearly discernable. Figure 4(c) shows that based on lateral scans across the middle of the image, bare and buried lines have comparable sharpness of approximately 70 nm. In fact, by averaging all linear scans across the lines, the sharpness was  $69 \pm 7$  nm for bare lines and  $70 \pm 13$  nm for buried lines. The present sharpness is comparable but not necessarily better than that of [3], because [3] buries the lines under a thicker oxide. Figure 4(c) shows also that the difference in contrast (signal magnitude) between buried lines and oxide is approximately half of that between bare lines and oxide. Had the oxide thickness not been known, it could have been estimated from the amount of the contrast degradation with the known dielectric constant of the oxide.



**Fig. 4.** SMM magnitude images of 390 nm-wide (a) bare and (b) buried aluminum lines. (c) Linear scans across both bare (—) and buried (---) lines.

Figure 4(c) shows that with a weaker signal, SNR is correspondingly worse for buried lines. SNR can be improved by averaging across adjacent linear scans, as will be illustrated for the scans in water. SNR may also be improved by averaging repeated scans or measurements (by VNA) at the expense of scan rate. Although presently the images formed by the  $S_{11}$  magnitude and phase are of comparable quality, this is not always the case. Depending on the detailed SMM working conditions, one can be significantly better than the other. For example, for different tips, samples, tip-sample distances, and ambient conditions, the resonant frequency can shift as will be illustrated for the case in water. The change of frequency can in turn change the loss and electrical length of the transmission line, and, hence, the magnitude and phase of  $S_{11}$ .

As mentioned earlier, water was used to simulate high- $k$  dielectric. Figure 5 shows the SMM phase image and linear scan over a 390 nm-wide bare line in water. It can be seen that although the line is still discernible, the signal and noise become comparable making it difficult to define sharpness from a single linear scan. However, the SNR can be significantly improved just by averaging a few adjacent scans as shown in Fig. 5(b). Statistically, a sharpness of  $69 \pm 13$  nm was obtained, which is comparable to the cases without water. This is apparently an order-of-magnitude improvement over the 700 nm sharpness we reported in [4].

The sharpness improvement over [4] is mainly due to the difference in the parasitic capacitance between the probe body

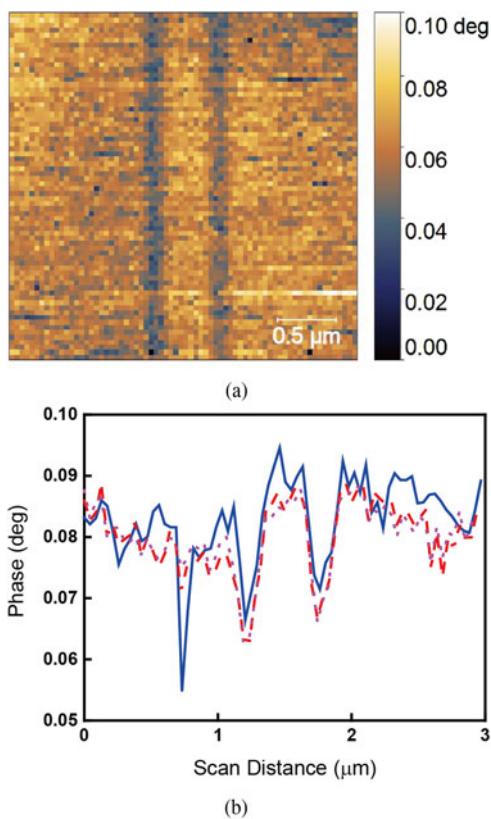


Fig. 5. SMM phase (a) image and (b) linear scans across an area of  $3 \mu\text{m} \times 3 \mu\text{m}$  ( $70 \times 70$  pixels) over a 390 nm-wide buried aluminum lines in water. In (b), averages across 6 (---) and 10 (...) adjacent lateral scans approximately 40 nm apart are shown for comparison with a typical single scan (—).

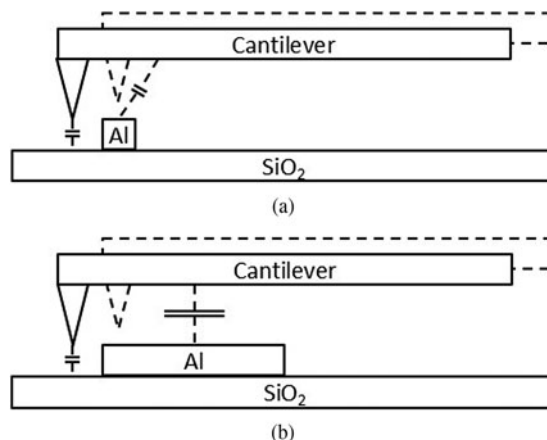


Fig. 6. Schematic illustration of the capacitive interaction when an SMM probe traverses (a) narrow and (b) wide aluminum lines embedded in silicon dioxide.

(cantilever) and the sample. Figure 6 illustrates schematically the capacitive interaction when a probe traverses an aluminum line embedded in silicon dioxide. In general, the capacitance can be divided into two parts, a sensing capacitance between the probe tip and the sample and a parasitic capacitance between the probe cantilever and the sample. Usually, with the tip in intimate contact with the sample and the cantilever suspended  $80 \mu\text{m}$  in air above the sample, the parasitic capacitance is relatively small even though the cantilever is much larger than the tip. However, with the air replaced by water, the parasitic capacitance increases drastically. This parasitic capacitance not only overwhelms the sensing capacitance, but also remains constant so long as the cantilever completely overlaps a wide aluminum line such as in [4] (Fig. 6(b)). In this case, the line is effectively being probed by the large ( $400 \mu\text{m} \times 60 \mu\text{m}$ ) cantilever instead of the sharp tip, which explains why the sharpness is approximately 600 nm in [4], much larger than the tip radius of 20 nm. In comparison, when the probe traverses a narrow line (Fig. 6(a)), both the sensing and parasitic capacitances change readily, resulting in a sharpness of 70 nm, which is not much larger than the tip diameter. Thus, counterintuitively, in water it is more difficult to probe a large feature than a fine feature due the large parasitic capacitance with the cantilever. This parasitic capacitance can be minimized by more complete shielding of

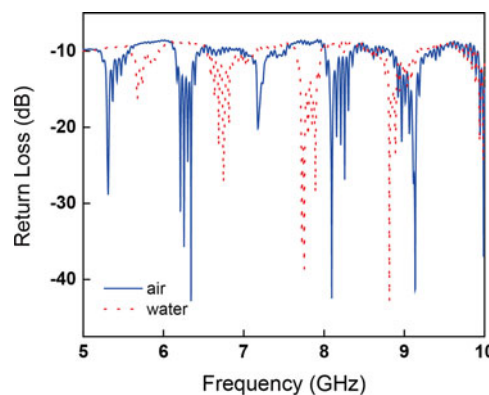


Fig. 7. Magnitude of reflection coefficient  $|S_{11}|$  (after subtracting the 30 dB amplification factor) from an SMM probe in air (—) and water (...) without touching any sample.

the microwave signal path all the way through the cantilever such as in a strip-line configuration [7].

For narrow lines, although water degrades the SNR, the sharpness remains approximately 70 nm as in air. This is very encouraging because it implies that SMM can also be used to non-invasively probe the internal structure of a live biological cell that needs to be kept in an aqueous solution as suggested by [8]. However, SMM of live biological samples presents additional challenges due to their soft and moving nature which need further development.

The present SMM image in water was obtained at 7.865 GHz instead of the typical 5.371 GHz. This is because the SMM uses an impedance matching network that works only at certain resonance frequencies. The resonance frequency shifted when the probe and the chip were immersed in water as shown in Fig. 7.

## Conclusion

SMM was successfully used to image CMOS interconnect lines as narrow as 190 nm and buried under Al<sub>2</sub>O<sub>3</sub> or water. Although water degraded the SNR significantly, it did not degrade the image sharpness. The sharpness remains approximately 70 nm in all cases. These results imply that SMM can be a promising technique for non-destructive nano-characterization of both CMOS interconnects buried under oxide and live biological samples immersed in water. However, quantitative characterization of the electrical properties of the samples awaits further development.

**Acknowledgement.** The project depicted is sponsored in part by the US Department of Defense, Army Research Laboratory under Grant No. W911NF-14-1-0665 and W911NF-17-1-0090, as well as Air Force Office of Scientific Research under Grant No. FA9550-16-1-0475.

## References

- [1] Turkane SM and Kureshi AK (2017) Emerging interconnects: a state-of-the-art review and emerging solutions. *International Journal of Electronics* **104**, 1107–1119.
- [2] Smoliner J, Huber HP, Hochleitner M, Moertelmaier M and Kienberger F (2010) Scanning microwave microscopy/spectroscopy on metal-oxide-semiconductor systems. *Journal of Applied Physics* **108**, 064315–1–064315-1.
- [3] You L, Ahn J-J, Obeng YS and Kopanski JJ (2016) Subsurface imaging of metal lines embedded in a dielectric with a scanning microwave microscope. *Journal of Physics D: Applied Physics* **49**, 045502–1–045502-11.
- [4] Jin X, Xiong K, Marstell R, Strandwitz N, Hwang JCM, Farina M, Göritz A, Wietstruck M and Kaynak M (2017) Scanning microwave microscopy of aluminum CMOS interconnect lines buried in oxide and water, European Microwave Conference (EUMC), Nuremberg, Germany.
- [5] Mai A and Kaynak M (2016) SiGe-BiCMOS based technology platforms for mm-wave and radar applications, International Conference on Microwave, Radar and Wireless Communications (MIKON), Krakow, Poland.
- [6] Ellison W (2007) Permittivity of pure water, at standard atmospheric pressure, over the frequency range 0–25 THz and the temperature range 0–100 °C. *Journal of Physical and Chemical Reference Data* **36**, 1–18.
- [7] Lai K, Kundhikanjana W, Kelly MA and Shen ZX (2008) Calibration of shielded microwave probes using bulk dielectrics. *Applied Physics Letters* **93**, 123105–1–123105-3.

- [8] Tuca S-S, Gramse G, Kasper M, Brinciotti E, Oh Y-J, Campagnaro GM, Badino G, Hinterdorfer P and Kienberger F (2015) Single *E-coli* bacteria imaged at 20 GHz frequency using the scanning microwave microscope (SMM). *Microscopy and Analysis* **29**(4), 9–12.



Xin Jin received the B.S. degree in Optical Science and Engineering from Fudan University, Shanghai, China in 2015. He is currently a Ph.D. student in electrical engineering at Lehigh University, Bethlehem, PA, USA. In 2016, he was a visiting Ph.D. student in Marche Polytechnic University, Ancona, Italy. He is currently involved in researches on the design and applications of scanning microwave microscope on both semiconductor devices and biological samples.



devices.

Kuanchen Xiong received the B.E. degree in Electronic Science and Technology from Southeast University, Nanjing, China in 2015. He then joined the research group of Professor James C. M. Hwang at the Department of Electrical and Computer Engineering, Lehigh University. His current research interest focuses on 2D semiconducting materials, CMOS-compatible processes, and nano-electronic



Roderick Marstell received his B.S. and M.S. degrees from California Polytechnic State University at San Luis Obispo in 2013. He is currently a Ph.D. candidate at Lehigh University in Dr. Nicholas Strandwitz's group. His research is focused on understanding the interdependence of Schottky barrier height and electrostatic charges in atomic-layer deposited oxides.



Nicholas C. Strandwitz joined the Lehigh University faculty in January 2013. He completed his B.S. in Engineering Science at the Pennsylvania State University in 2004. He then earned his Ph.D. from the Materials Department at the University of California, Santa Barbara with Professor Galen D. Stucky. He then conducted postdoctoral work at California Institute of Technology working with Professor Nathan S. Lewis. His research interests include new chemistries and techniques in atomic-layer deposition and interfacial electronic properties between semiconductors and metal oxides.



James C. M. Hwang received the B.S. degree in Physics from the National Taiwan University, Taipei, Taiwan in 1970, and the M.S. and Ph.D. degrees in Materials Science and Engineering from Cornell University, Ithaca, New York, in 1976 and 1978, respectively. Since 1988, he has been Professor of Electrical Engineering and Director of Compound Semiconductor Technology Laboratory at Lehigh University, Bethlehem, Pennsylvania. Prior to that, he spent 12 years at IBM, AT&T, GE, and GAIN. He cofounded GAIN and QED; the latter became a public company (IQE). His current research interests include

scanning microwave microscopy, two-dimensional atomic-layered materials and devices, and microwave characterization of individual biological cells.



**Marco Farina** received the M.S. degree in 1990 and the Ph.D. degree in 1995, both in Electronic Engineering from the University of Ancona, Italy. He is currently Professor of electromagnetics at the Marche Polytechnic University, Ancona, Italy. He is a Senior Member of IEEE and a Technical Committee Member of the IEEE MTT Society TC-25 RF-Nanotechnology. He authored the electro-

magnetic simulation software EM3DS, currently used by a number of institutions and embedded in the National Instruments tool Microwave Office. Dr. Farina designed and realized a hybrid scanning tunneling microscope/scanning microwave microscope. His research interests include electromagnetic modeling of passive and active structures, scanning probe microscopy, nanotechnology and measurement techniques.



**Alexander Göritz** received the Dipl.-Ing. degree in Electrical Engineering (microelectronics-semiconductor technology) from the Technical University Dresden, Germany, in 2011. In 2012, he joined the Technology Department of IHP Microelectronics, Frankfurt (Oder), Germany and started working on the development of micro-electromechanical systems (MEMS) with thin-film wafer-level encapsulation for mm-wave applications. He applied and optimized the HF

vapor-phase-etching process to release the finished MEMS devices. Since 2014 he has been involved in the creation and application of back-end-of-line (BEOL) processes to realize cost-efficient passive devices.

vapor-phase-etching process to release the finished MEMS devices. Since 2014 he has been involved in the creation and application of back-end-of-line (BEOL) processes to realize cost-efficient passive devices.



**Matthias Wietstruck** received his diploma in Microsystems Technology in 2009. Since 2010, he has been with IHP Microelectronics, Frankfurt (Oder), Germany. Since 2015 he is leading the group “Heterointegration of Devices and Technologies” as part of the research program “Technology for wireless and broadband communication”. His research interest is in the field of monolithic and heteroge-

neous integration of millimeter-wave BiCMOS RF-MEMS, through-silicon vias, temporary and permanent wafer bonding applications, and BiCMOS embedded microfluidics.



**Mehmet Kaynak** received the B.S. degree from the Electronics and Communication Engineering Department of Istanbul Technical University, Turkey in 2004, the M.S. degree from the Microelectronic Program of Sabanci University, Istanbul, Turkey in 2006, and the Ph.D. degree from Technical University of Berlin, Germany in 2014. He joined the technology group of IHP Microelectronics, Frankfurt (Oder),

Germany in 2008. From 2008 to 2015, he led the MEMS development at IHP. Since 2015, he is Head, Technology Department at IHP. He is an Adjunct Professor at Sabanci University.